Wear 271 (2011) 2651–2659

Contents lists available at ScienceDirect

Wear

journal homepage: www.elsevier.com/locate/wear

Short communication

Construction of a tribocorrosion test apparatus for the hip joint: Validation, test methodology and analysis

M.T. Mathew[a,*], T. Uth[a], N.J. Hallab[a], R. Pourzal[b], A. Fischer[b], M.A. Wimmer[a]

[a] Section of Tribology, Department of Orthopedic Surgery, Rush University Medical Center, Chicago, USA
[b] Department of Material Science and Engineering II, University of Duisburg-Essen, Duisburg, Germany

ARTICLE INFO

Article history:
Received 12 September 2010
Received in revised form 12 January 2011
Accepted 12 January 2011

Keywords:
Tribocorrosion
Normal load
Metallic implants
Synergism

ABSTRACT

In biomedical research, because of the critical nature of corrosion within the environment of motion and interactions of weight bearing surfaces, scientists and engineers have shown a growing interest in the area of "*tribocorrosion*". Fundamentally, tribocorrosion combines the disciplines of tribology and corrosion and their concurrent exchanges. Principles of tribocorrosion are applied in a range of industries including the offshore, space and biomedical (for example, dental and orthopedic) industries.

One of the challenges in tribocorrosion research is the lack of standard testing equipment and methodologies, particularly in its bio-medical applications. Many investigators and research laboratories are engaged in modifying their existing classical tribology apparatus, whether they are commercially available or customized tribometers, to integrate electrochemical monitoring.

The current work is focused on developing a tribocorrosion test apparatus to model the contact situation of artificial hip joints with particular attention on possible erroneous issues that could arise in such a system. The test system facilitates studies on the tribocorrosion behavior of implant metals or coatings as a function of diverse tribological and electrochemical parameters, and allows monitoring temperature, pH and dissolved oxygen level during testing. Initial results on the HC CoCrMo alloy in bovine calf serum (BCS), indicate that the proposed system is reliable and useful for the investigation of tribocorrosion behavior of implant materials. Electrochemical impedance spectroscopy tests (EIS) are employed before and after the sliding tests. The usefulness of such tests in understanding the changes in the surface chemistry and corrosion kinetics are explained, with the help of optimum EIS models. An attempt has also been made to highlight the relevance on wear quantification methods and possible ways to analyse the synergistic interactions of wear and corrosion for the biomedical tribosystems in orthopedics and dentistry.

1. Introduction

Tribocorrosion is a multidisciplinary research area that has recently started to gain importance in many applications ranging from off-shore industry to biomedical engineering. "*Tribocorrosion*" is defined as an irreversible transformation of a metal/alloy resulting from simultaneous physico-chemical and mechanical surface interactions in a tribological contact [1]. The beneficial and detrimental effects observed by tribocorrosion interactions will assist in the selection of materials, the design of components and the selection of operational variables. Because of its practical and economical importance, a growing number of research laboratories focus their work on this area [2–6].

A recent review [7] of tribocorrosion research during the last decade (1996–2006) highlighted the implications of tribocorrosion research for biomedical applications, and noted that more than half of the reported investigations are related to biomedical implants in dentistry and orthopedics. Tribocorrosion investigation of artificial hip joint bearings is important, especially in the case of metal-on-metal (MoM) bearings that are currently considered as an alternative to metal–polymer (MoP) and ceramic-on-ceramic (CoC). Results of the reported studies show that the wear rate of MoM joints is 10-100 times lower than that of conventional MoP joints. Other benefits of MoM joints are the simple fabrication processes, high fracture toughness, and the ability to use large femoral heads to avoid the risk of post-operative instability [8,9].

Metallic implants in living organisms are constantly exposed to biological fluids, living cells having their own metabolism, uneven distribution of dissolved oxygen, which creates a corrosive environment. The behavior of the metals in such an environment may change significantly. For example, the high corrosion resistance

* Corresponding author. Tel.: +1 312 942 8310; fax: +1 312 942 4491.
E-mail addresses: mathew_t_mathew@rush.edu, mathewtmathew@gmail.com (M.T. Mathew).

0043-1648/$ – see front matter © 2011 Elsevier B.V. All rights reserved.
doi:10.1016/j.wear.2011.01.085

of CoCrMo alloy in air or aqueous conditions is reduced in the body environment, where the pH value is approximately 7.4 [9]. Wear debris and metal ions that are released *in vivo* can have negative effects on the patients' health, including periprosthetic bone loss leading to aseptic loosening, inflammatory responses and adverse tissue reactions [9–11]. Theoretical systemic effects of high ion levels include metal hypersensitivity, metal toxicity and carcinogenesis [10]. Because these effects likely intensify with increasing exposure time, they pose serious health issues especially on younger and active patients. Further, the biocompatibility of metals and alloys used for bearings in hip arthoplasties normally relies on the stable passive film. It is possible that this film breaks down due to mechanical action without being reformed immediately. In addition, the dissolved oxygen level of the surrounding media plays an important role in stable film growth. The metal surface might form a layer (known as a tribochemical reaction layer [11–14]) by reacting with proteins and other contents of the surrounding media. Therefore, tribocorrosion studies could provide valuable information on the performance of artificial metal joints and how the scope of MoM bearings could be extended.

One of the challenges in tribocorrosion research is the lack of standard test systems. A specially designed tribocorrosion apparatus would be helpful in improving electrochemical interfacing and yield reliable results. The purpose of this study was to design, develop and fabricate a tribocorrosion set-up for hip joint application. First, existing tribocorrosion test systems used by various laboratories were reviewed. Then, general design considerations in constructing a tribocorrosion set-up were formulated. The advanced facilities of the test system, such as monitoring temperature, pH and dissolved oxygen levels are explained. Finally, a pilot study was conducted to demonstrate the reliability of the developed system and to compare results obtained with the developed system to those from other laboratories/test systems.

2. Tribocorrosion test system

2.1. Basic methodology

The basic test system commonly used in tribocorrosion tests is the pin-on-flat system as illustrated in Fig. 1. The tribological set-up interfaces with an electrochemical testing system by using a potentiostat. The interfacing system consists of a three electrode arrangement, namely, reference electrode (RE), counter electrode (CE) and working electrode (WE). Tribological studies deal with mechanical parameters describing the interaction between articulating surfaces.

The articulation generates frictional forces that may cause the surface to deform and lead to wear. Available electrochemical techniques including open circuit potential (OCP), potentiodynamic test (PD), potentiostatic test (PS) and electrochemical impedance spectroscopy test (EIS) are suitable for studying the tribocorrosion process. These techniques allow monitoring and controlling the electrochemical test conditions during sliding and assist in quantifying the relationship between corrosion and total wear volume.

2.2. Hip joint as a tribocorrosion system

In a hip joint, there are many possibilities for tribocorrosion events at the implant surface. Next to articulation between the femoral head and acetabulum, micro-movement between the femoral stem and cortical bone can occur. While retrieved implants have provided evidences of failure modes caused by corrosion, influencing parameters and their interactions are poorly understood [8,9].

Laboratory tests using artificial joint simulators (*in vitro* tests) are currently the best solution for understanding the system. Wimmer et al. [15,16] constructed a unique type of simulator with a conforming pin-on-ball contact condition that mimics the structural and mechanical aspects of the natural hip joint. In this study, the tribocorrosion set-up is constructed to structurally mimic the simulator allowing for comparisons of results from both systems and collection of baseline data for further analysis.

Previous studies on the tribocorrosion behavior of implant materials employed in the artificial hip joints can be divided into different classes of tribocorrosion systems including fretting-corrosion [17–19], sliding wear-corrosion [20] and microabrasion-corrosion [21–23]. The studies have tested different couples of MoM or MoC (metal-on-ceramic) in simulated physiological solution to replicate the joint conditions. However, to date information on tribocorrosion of a pin-on-ball system simulating hip joint articulations and mechanisms is not available.

2.3. Tribocorrosion systems in the literature

Most investigations on tribocorrosion have utilized an available tribometer with appropriate modifications to integrate an electrochemical set-up. The main advantage of such arrangements is the well defined and controlled tribological set-up. However, the disadvantages include (i) potential artifacts on the proper functioning of the tribometer, (ii) difficulties in data collection, particularly in synchronizing the data from corrosion and tribological events, and (iii) potential difficulties in correlating the results and evolution of the selected parameters. Some test set-ups used for tribocorrosion studies are listed in Table 1. Additional details of these systems are provided below:

(a) *Pin/ball on disk rotating (one direction):* unidirectional sliding of a ball or pin against a plate (Stack and Chi [24]).
(b) *Ball (or pin) on plate (reciprocating):* in this system, a ball or pin (held by a vertical holder) is sliding back and forth using the same wear track against the plate under reciprocating conditions. This is the most commonly used tribocorrosion set-up (Yan et al. [20,25], Hendry and Piliar [19], Celis et al. [26–31], Mischler et al. [32–37], Azzi et al. [38], Duisabeau et al. [39], Mathew et al. [40] and Ferreira et al. [41]).
(c) *Microabrasion test system (ball on plate):* in a microabrasion test system the ball is rotating about one axis against a vertical plate and allows the insertion of third bodies (Stack et al. [22], Wood et al. [21]).
(d) *Cylinder on-bar:* in this system, the cylinder moves against the bar (Pourzal et al. [42]).
(e) *Ring-on-disk*: in this system, the disk is fixed and the ring is rotating. The electrochemical interfacing is achieved like in the other systems (Serre et al. [43]).
(f) *Special apparatus*: a few research laboratories have developed special tribocorrosion experimental set-ups to replicate practical applications. For instance, a setup by Geringer et al. [17] to study the tribocorrosion events of the hip joint femoral stem and the cortical bone. Hallab et al. [18] developed a special tribocorrosion (fretting-corrosion) system for hip joint taper junctions. Rocha et al. [30] developed a special set-up for tribocorrosion test for dental applications.

In general, this review shows that researchers used different tribocorrosion test systems based on the specific aims of their study. The contact configurations, type and movements of the counterbody and nature of the test system itself will have an influence on the results generated. Hence, the influence of the type of tribocorrosion system should not be neglected in inter-laboratory comparisons. Further, the selection of a test system for a specific

Table 1
Types of available tribocorrosion test systems.

Tribocorrosion system	S. no	Source	Type of tribocorrosion	Basic tribometer	Interest of the study	Sample	Electrolyte	Movement
(a) Pin on disc (uni-direction)	1	Stack and Chi [24]	Sliding-corrosion	Customized tribometer	Industrial application	Steel and alumina	Sodium carbonate/bicarbonate solution	Disk is rotating against the pin
	2	Manish et al.	Sliding-corrosion	Customized tribometer	Industrial application	Steel and alumina	Sodium carbonate/bicarbonate solution	Disk is rotating against the pin
(b) Ball on plate (reciprocating)	3	Yan et al. [20–25]	Sliding-corrosion	Customized tribometer	Biomedical: orthopedic	CoCrMo alloy	BCS	SiN ball-reciprocating
	4	Azzi et al. [38]	Sliding	Customized tribometer	Biomedical: coatings performance	Ti and TiN	Ringer solution, BCS	Ball-reciprocating movement
	5	Berradja et al. [31]	Sliding-corrosion	Customized tribometer	Effect of load and frequency	Stainless steel	Ringer solution	Ball is reciprocating
	6	Basak et al. (2006) [29]	Sliding-corrosion	Customized tribometer	Industrial application: To study the behavior of new materials	SS, nano-structured WC-Co, FeCu/WC-Co coatings	Hanks solution	Ball is reciprocating
	7	Hendry and Piliar [19]	Fretting-corrosion	Customized tribometer	Biomedical: PVD surface-modified implant alloy	Co-alloy Ti6Al4V	Hanks solution	Plate is reciprocating
	8	Barril et al. (2004) [33–35]	Fretting-corrosion	Customized tribometer	Biomedical:	Ti6Al4V	NaCl solution	Plate is moving
(c) Pin on plate (reciprocating)	9	Mathew et al. (2006) [40]	Sliding-corrosion	Plint TE-67/E	Thin films,	TiCO films	Artificial sweat	Plate is moving
	10	Fernades et al. (2005) [41]	Sliding-corrosion	Plint TE-67/E	Thin films	TiN films	Artificial sweat	Plate is moving
	11	Sonia et al. [41]	Sliding-corrosion	Plint TE-67/E	Thin films,	ZrNO films	Artificial sweat	Plate is moving
(d) Microabrasion	12	Wood et al. [21]	Microabrasion-corrosion	Microabrasion	Biomedical, load, potential	CoCrMo-alloy	BCS	Ball is rotating (uni-direction)
	13	Stack et al. [22]	Microabrasion-corrosion	Microabrasion	Biomedical, x	Mild steel	Sodium carbonate/bicarbonate solution	Ball is rotation (uni-direction)
(e) Cylinder on bar	14	Pourzal et al. [42]	Sliding-corrosion	Customized tribometer	Biomedical	CoCrMo alloy	Physiological solution, BCS	Bar is moving
(f) Ring-on-disk	15	Serre et al. [43]	Sliding-corrosion	Customized tribometer	Industrial	Graphite and Ti alloy	Sea water	Ring is moving, disk is fixed.
(g) Special type of set-up	16	Geringer et al. [17]	Fretting-corrosion	Special set-up	Biomedical-femoral stem	316 SS and PMMA	Ringer solution	Special set-up
	17	Duisabeau et al. [39]	Fretting-corrosion	Special set-up	Biomedical-femoral stem	Head-Ti–6Al––4V Neck-SS316 steel	Ringer solution	Special set-up
	18	Hallab et al. [18]	Fretting-corrosion	Special set-up	Biomedical-femoral head	CoCrMo alloy-head	Ringer solution	Special set-up
	19	Luis et al. [30]	Sliding-corrosion	Special set-up	Dental application	CpTi	Artificial saliva	Ball is moving

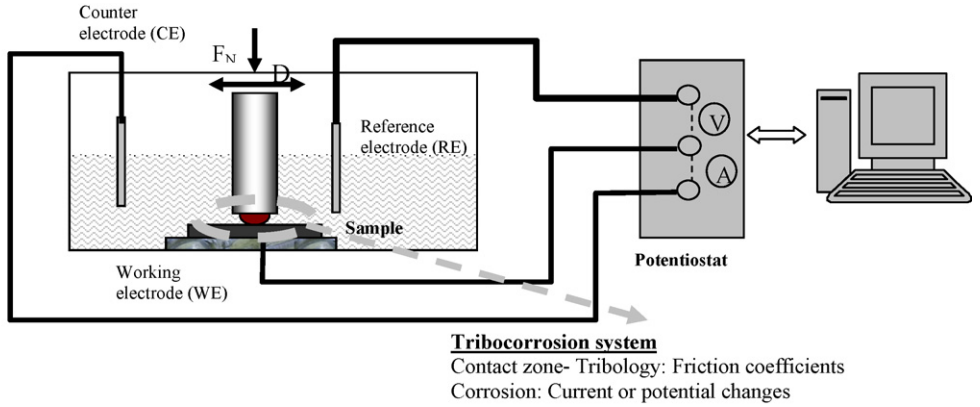

Fig. 1. Basic methodology used in the tribocorrosion system.

study primarily relies on the contact conditions and characteristics of the mechanical parameters (including load, frequency and velocity) in relation to practical applications. In the course of this analysis, a set of design considerations are formulated and listed in Appendix A.

3. Details of the developed tribocorrosion test apparatus

In the current work, a tribocorrosion system with a pin-on-ball configuration was designed and constructed for hip joint application. In this set-up, the tribological contact was comprised a pin (horizontal) in contact with a ball, which underwent oscillatory rotational motion. However, because of practical limitations, the pin is always fixed and the other side of the ball is held by a polymer support made from UHMWPE (ultra high molecular weight polymethylene) to electrically disconnect the ball from the load frame.

3.1. General description

The assembled tribocorrosion system is shown in Fig. 2(a)–(c). The important components of the systems are (i) a tribocorrosion cell, (ii) an electro-mechanical vertical load frame (UTS, Germany), (iii) a pneumatic horizontal load frame, and (iv) support bearings. The tribocorrosion cell is placed between the two support bearings and holding the chemical solution or electrolyte. The vertical load frame allows for precise up and down movement of the ball holder. A rotary actuator, mounted on the traverse of the vertical load frame, generates the cyclic rotation of the ball. A torque sensor (Model: TRT-200, supplied by Transducer Technique, Temecula, CA, USA) was placed in line with the ball holder. Using a polymer connector/bush ensures that the ball holder is electrically isolated from the load frame (test system). The left and right bearings bear the shaft carrying the tribocorrosion cell. The horizontally aligned pneumatic load frame is used to apply the axial load. The load cell (ELPM-T3M-1.25KN, Entran Ltd, Hampton, VA, USA) is located in line with the bearing axis and measures the applied load.

3.2. Tribocorrosion cell and data collection

The central component of the test system is the tribocorrosion cell which consists of a double-walled cage made of acrylic glass (Fig. 2(a) and (c)) allowing the circulation of water (heated water bath system) to maintain a constant solution temperature inside the tribocorrosion cell. Through the cavity at the top of the tribocorrosion cell, the ball holder is inserted so that the ball comes into contact with the pin on one side and with polymer support made from UHMWPE on the other side. Electrodes for the electrochemical test are also inserted into the solution. A standard calomel electrode (SCE) is used as reference electrode and a graphite rod as counter electrode. The sample to be tested (pin) acts as a working electrode (WE). To maintain consistent test conditions, the electrodes are always positioned in the same locations inside the cell. Finally, the contact zone is clearly visible from Fig. 2. The pin surface in the vicinity of the ball is exposed to the solution and in contact with the ball. The pin is placed in the tribocorrosion cell through the polymer pin holder, and special care is taken to avoid any likelihood of contact with the solution except at the surface, which is in non-conforming contact with the ball.

Dissolved oxygen appears to have an important role for corrosion conditions in biomedical applications [44]. Hence, a dissolved oxygen meter (Laserlab Inc, NY, USA) is used to monitor the dissolved oxygen level during the test. The system also allows for the insertion of a dissolved oxygen level electrode into the tribocorrosion cell.

The applied load, the angle of rotation of the ball (amplitude of oscillations) and the torque are monitored by a DARTEC 9690 controller and the software package Workshop 9600 (Zwick, Germany).

A Gamry potentiostat is used in corrosion measurements using a three electrode system. The potentiostat can be used for standard corrosion tests including open circuit potential, potentiodynamic and potentiostatic tests, electrochemical impedance tests. The standard protocol used for this test consists of an initial stabilization period, sliding period (based on number of cycles) and final stabilization [40]. The wear volume loss can be estimated using mathematical/empirical equations or imaging techniques.

4. Details of the pilot study

To validate the test system, a pilot study was carried out on CoCrMo alloy samples in the presence of 2.4% NaCl solution (a common electrolyte used for electrochemical studies) and bovine calf serum solution (BCS, proteins content is 30 g/L) the lubricant of choice for hip wear testing. The tribological pair consisted of cylindrical CoCrMo pin, 12 mm diameter and 7 mm thickness with a flat face articulating against a ceramic ball of 28 mm diameter at frequency of 1 Hz and amplitude of 15°. Because a flat surface was in contact with a convex surface, the Hertzian pressure distribution was estimated. A load of 16 N is required for a 350 MPa of Hertzian contact pressure, which was used in the previous studies [45,46].

Two types of corrosion tests are recommended for tribocorrosion experiments. *(1) Free potential*: during this test the evolution of potential is measured, where the anodic cathodic reaction rates are equal and no current flows to or from the electrode. *(2) Potentiostatic test*: a specific potential is applied (typically anodic, $E_{passive}$, E_{corr} or any selected potential, these potentials can determined

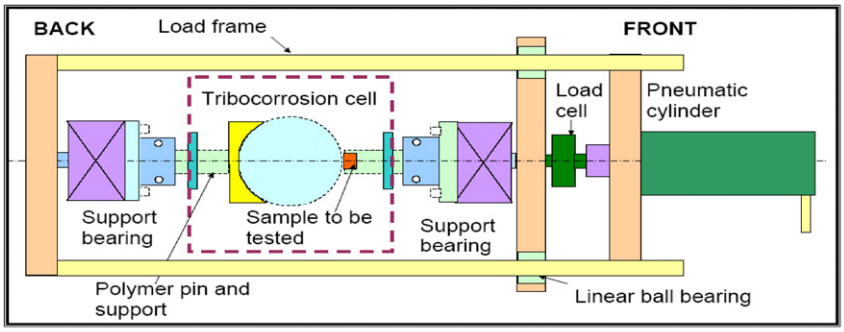

(a) Assembled view of the developed tribocorrosion set-up

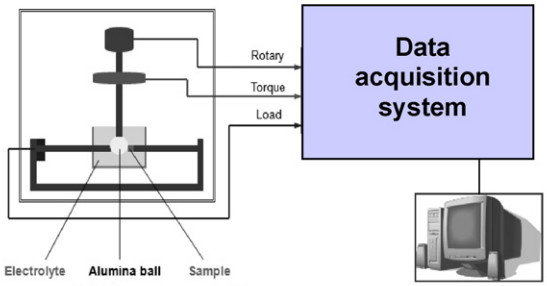

(b) Data acquisition system

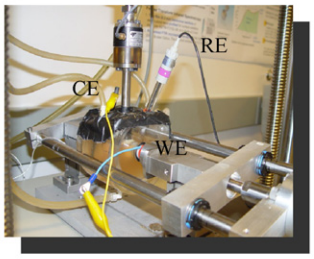

(c) Close picture of the tribocorrosion cell and electrode positions

Fig. 2. Assembled view of the entire tribocorrosion set-up.

from the potentiodynamic curves by using Tafel's methods) and the evolution of the current is monitored. The selection of potential is based on the potentiodynamic curves derived from the basic corrosion tests (with no tribological events).

Initial tests (Test 1) were conducted at free potential conditions. During the test, the evolution of electrode potential was monitored for a period of 1000 cycles. Subsequently, a potentiostatic condition was selected, and the evolution of current was monitored at E_{corr} (Test 2). Next, a potentiostatic test (Test 3) at a potential of E_{corr} was conducted at the identical conditions of Test 2 but in BCS solution for comparison with 2.4% NaCl solution. Finally, to confirm the suitability of the test system for long duration tests and to verify the reproducibility of the test results, two tests were conducted for 100 K cycles in BCS solution, under free potential (Test 4) and potentiostatic conditions (Test 5).

5. Results and discussion

5.1. Evolution of corrosion potential and friction coefficient values as a function of sliding time

5.1.1. General trend during 1000 cycles

The evolution of corrosion potential and friction coefficient as a function of time is shown in Fig. 3(a). The evolution of potential exhibited a trend towards reduced values during sliding which is in agreement with previous work [24,37]. After completion of the sliding motion, the potential returned to the initial value similar to what has been observed during the final stabilization. In contrast, the evolution of friction coefficient values appeared to remain constant (ranging from 0.33 to 0.39) during the test period of 1000 cycles.

It should be noted that the potential measurement was based on the potential differential spontaneously established between the working electrode (WE) (i.e., sample) and a reference electrode (RE). The potential clearly showed a cathodic increase (moving towards cathodic potentials or cathodic shift) with increasing duration of sliding. Generally, the decrease in corrosion potential indicates an increase in corrosion tendency of the material surface. Possible reasons for this result include removal of the passive films and increase in exposed area during sliding. Further, the measured corrosion potential reflects upon the galvanic coupling of two distinct surface states of the metal; (a) the passive metal (unworn area) and (b) the bare metal (worn area) may have been exposed to the solution by abrasion of the passive film. When the sliding stopped, the corrosion potential attained the initial value because of the formation of passive (oxide) film under stable condition.

Fig. 3(b) shows the evolution of potential for five cycles. It is interesting to note the definite pattern of potential variation for each cycle.

Ponthiaux et al. [27,28] theoretically identified the four key parameters affecting the evolution of potential during the sliding: (i) the intrinsic corrosion potentials of the worn and unworn surfaces; (ii) the ratio between the worn and unworn surface areas; (iii) the relative position of worn and unworn areas; (iv) the mechanisms and kinetics of the involved reactions. Unfortunately, all of the above parameters are difficult to define and control. In this study, the worn area was partially/fully covered by the rotating ball. Further, the nature of the unworn area was unpredictable because it could react with surrounding solution and form a passive film through the electrochemical reactions. This film was formed in an organic environment containing proteins and lubricants depending on the duration of exposure time and surface conditions.

In their studies on the fretting corrosion of Ti6Al4V, Duisabeau et al. [39] also found the interdependency of free corrosion potential and dissipated energy. The fretting causes a reduction in free potential which increases with dissipated energy level. In this study, the tribological system resembled fretting tribological conditions (although this is not a fretting test) because the contact zone/area

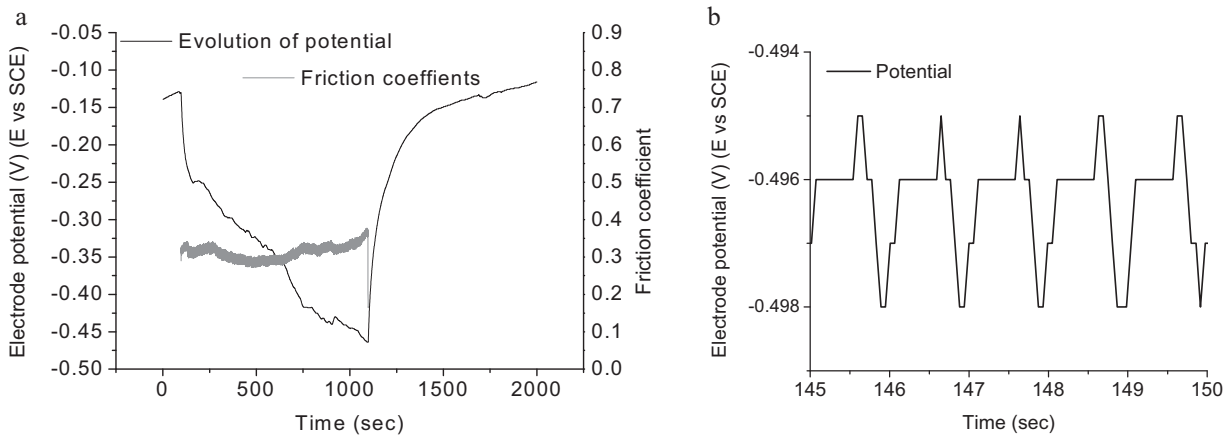

Fig. 3. Results of the pilot study with 2.4% NaCl solution. (a) Evolution of electrode potential and friction coefficient for 1000 cycles; (b) evolution of electrode potential for 5 cycles.

was always covered by the ball. Hence, the passive film is continuously damaged leading to "surface depassivation". This leads to significant metal dissolution and reduction in corrosion potential. Consequently, knowledge about the local state of the surface is critical for a precise physical interpretation of the relations and material degradation. Recent techniques using microelectrodes or the scanning reference electrode technique (SRET) may provide more information on the potential distribution on surfaces including the worn and unworn surfaces [7].

5.2. Evolution of current and friction coefficients at potentiostatic conditions

The evolution of the current and friction coefficient at E_{corr} is shown in Fig. 4(a). During rubbing in a potentiostatic condition (E_{corr}), the current displayed a clear increasing trend. Possible reasons for this observations include the increase in surface area that was exposed to the solution during the sliding motion and elimination of the passive films, which increased over-all corrosion current.

The results of tests in bovine calf serum (BCS; Test 3) are shown in Fig. 4(b). Interestingly, the evolution of current as a function of time shows steady state trend. This result is in contrast to the results for 2.4% NaCl solution (Fig. 4(a)) that shows a gradual increase as a function of the sliding duration. In addition, friction coefficient values were approximately half of those for 2.4% NaCl solution. These results demonstrate the influence of protein solution on the tribocorrosion behavior (for example, lubrication and third body), which need to be further investigated in subsequent studies.

It is speculated that in BCS, proteins can get adsorbed onto the negatively charged surface, i.e., the cathode (undamaged specimen surface), and/or the counter electrode may have blocked the mass transport of reduction reactants. This may have resulted in a diminished reduction process which in turn could have hindered the anodic process.

5.3. Estimation of weight loss

Optical images of a typical wear scar after 1000 cycles are shown in Fig. 5 and show that the test generated a spherical wear scar with well defined boundaries.

A sample of the solutions was extracted at each interval and analyzed for metal content using mass spectroscopy with coupled plasma technique (high resolution ICP-MS). Fig. 6 shows the evolution of Co and Cr content as a function of number of cycles at free potential (Mo particles were below the detection limit of 0.05 mg/kg).

Fig. 7 shows a comparison of weight loss estimations using two methods, namely, profilometric method and determination of total metal content. Initially, from the wear scar profile, the weight loss was estimated, as displayed in Fig. 7, marked as (A). The total metal content was determined from the Co, Cr, Mo distributions in the extracted representative solution after the test (marked as (B) in Fig. 7). There was good agreement between both techniques, indicating the validity of the test set-up and weight loss determinations. The small difference between both values could be

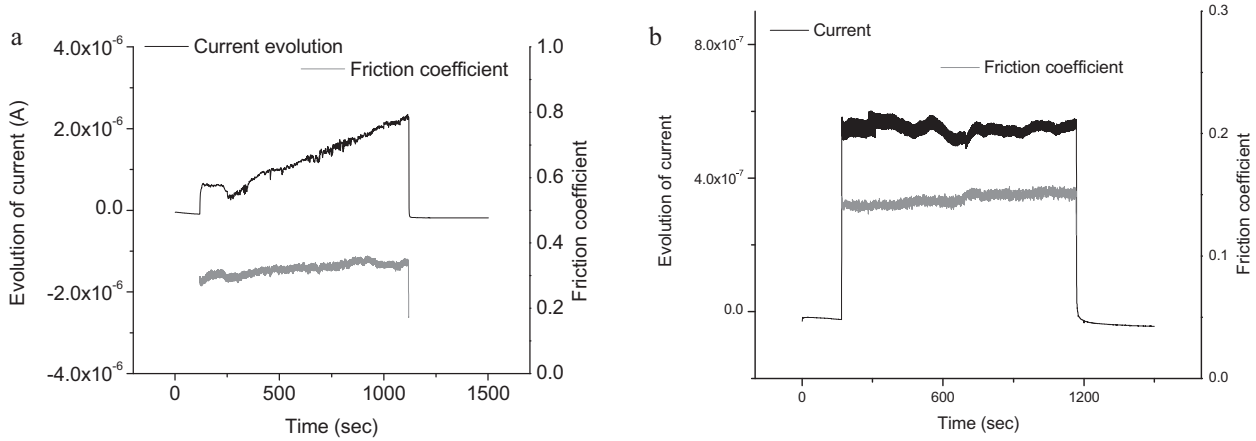

Fig. 4. Results of the pilot study with BCS solution: evolution current and friction coefficient for 1000 cycles at E_{corr}.

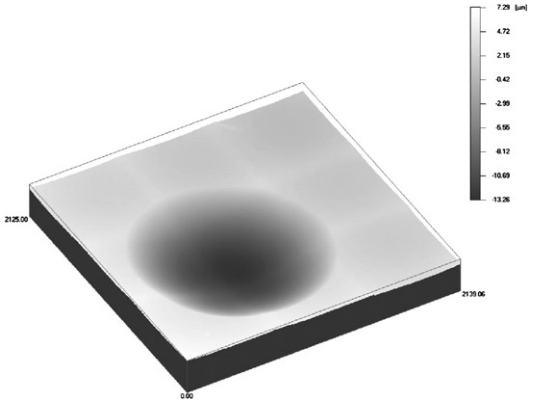

Fig. 5. Optical image of the wear scar obtained – three dimensional image of the wear scar.

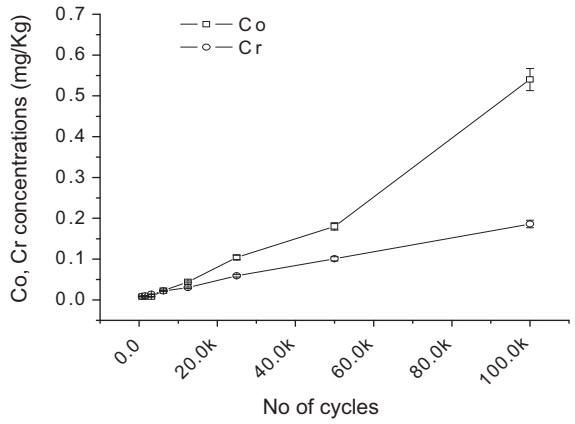

Fig. 6. Distribution of the Co and Cr particles from the chemical analysis (Test 4).

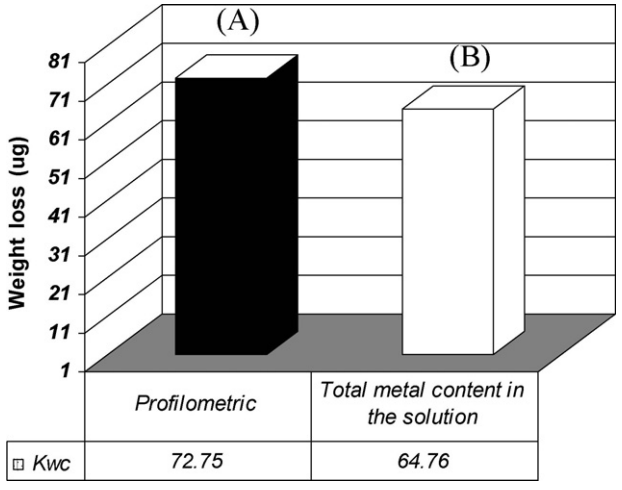

Fig. 7. Comparison between weight loss estimation by wear scar profilometry and total metal content (Test 4).

related to adhering wear particles to the counter body during the operation.

5.4. Reproducibility of the results and comparison with other test systems

In order to confirm the reproducibility the results from the tests, three consecutive trials (Test 5) were conducted under a potentiostatic condition (at −0.28 V *vs* SCE, other parameters are similar to Test 4) and results are displayed in Table 2. The developed tribocorrosion test system exhibited satisfactory repeatability with a standard error of 20.2 μg and the coefficient of variation of 20.7%.

Table 2
Weight loss estimation in a potentiostatic static test, (Test 5) illustrating the reproducibility of the test results.

Tests	Weight loss [μg]	Average weight loss [μg]	Standard deviation [μg]	Standard error [μg]
$n=1$	162.8			
$n=2$	210.8			
$n=3$	142.2	172.2	35.7	20.2

Table 3
Comparison of wear coefficient (k) with two other tribocorrosion systems from literatures [25,47].

Three tribocorrosion test system	Wear coefficient (k) in μg/Nm
New tribocorrosion system	7.08E−03
Yan et al. [25] (sliding-corrosion system)	1.50E−02
Stack et al. [47] (microabrasion–corrosion system)	5.39E−03

An attempt has also been made to validate the reliability of the test system, by comparing the wear coefficient (k) values (see Table 3) with two other tribocorrosion systems namely, a reciprocating sliding-corrosion system (Yan et al. [23–25]) and a microabrasion corrosion test system (Stack et al. [47]). Test conditions were similar (sliding distance and load) with the same material couples (CoCrMo alloy-alumina). The wear coefficient was estimated by

$$k = \frac{\text{Total weight loss (g)}}{\text{load (N)} \times \text{sliding distance (m)}}$$

As shown in Table 3, the calculated wear coefficient k was in the same order of magnitude as those reported earlier. The evolution of in situ electrochemical parameters (potential or current) as a function of sliding time were comparable to previous work, too [20,40]. Hence, the system is reliable in indicating electrochemical responses in association with the tribological events during the tribocorrosion process (see Fig. 4(a) and (b)) and the output is comparable with previous studies in literature. Investigations using this system may contribute to a better understanding of the synergistic interactions of wear and corrosion and categorize the possible mechanisms involved in such complex process.

5.5. Limitations and future work

The current test set-up was specifically designed for biotribocorrosion studies in total hip replacement. One of the limitations is that the set-up relies on two bearings, i.e. a ceramic-polymer articulation and the ceramic-metal articulation (Fig. 2), to apply the normal load. Such a configuration, however, allows precise friction measurements without crosstalk effects [48]. Hence, the normal load can be varied during the test, without affecting friction measurements. For this, a pneumatic cylinder system is used which is also helpful to compensate any load reduction during linear penetration of the ceramic ball into the counterface. Another limitation is that the ceramic-on-metal articulation is not a bearing couple in clinical use. However, the ceramic or inert counter body is necessary in the current set up (Figs. 1 and 2) to monitor and control the electrochemical measurements of the tested metal sample.

In future, studies are planned that will consider various electrochemical and mechanical parameters with a structured CoCrMo surface to test whether such surfaces can enhance the formation of a dynamic tribo-chemical reaction layer (Wimmer et al. [14,48]) during tribological interactions between counter bodies in the pres-

ence of biological solutions. Other materials combinations also will be considered. The influence of proteins and other components of synovial fluid on the tribocorrosion behavior of the implant materials will be studied in detail.

6. Conclusions

In this work a new tribocorrosion test system was designed and constructed specifically for hip joint applications. A review of the existing tribocorrosion apparatus in the literature has been provided. The results of a pilot study were discussed

The following conclusions can be drawn:

- The construction of a tribocorrosion set-up requires special attention, and a set of design considerations have been formulated.
- The developed system is appropriate for tribocorrosion investigations of implant materials and for simulating the hip joint.
- Evolved electrochemical parameters and mechanical events were comparable to those previously reported in the literature.
- Thorough knowledge of the test system dynamics and configurations of the tribological contacts is critical for the analysis and interpretation of results.

Acknowledgements

Partial financial support was provided by Zimmer GmbH, Winterthur, Switzerland. The authors would like to thank Mr. Eric Schmidt (University of Illinois at Chicago) for helping with design and construction of the test apparatus. Acknowledgments also go to Dr. Thomas Pandorf of Ceramtech, Plochingen, Germany for providing ceramic heads and Ms. Anne Mündermann for the fruitful comments and editorial assistantship with the manuscript.

Appendix A. Flow chart for developing a tribocorrosion test set-up

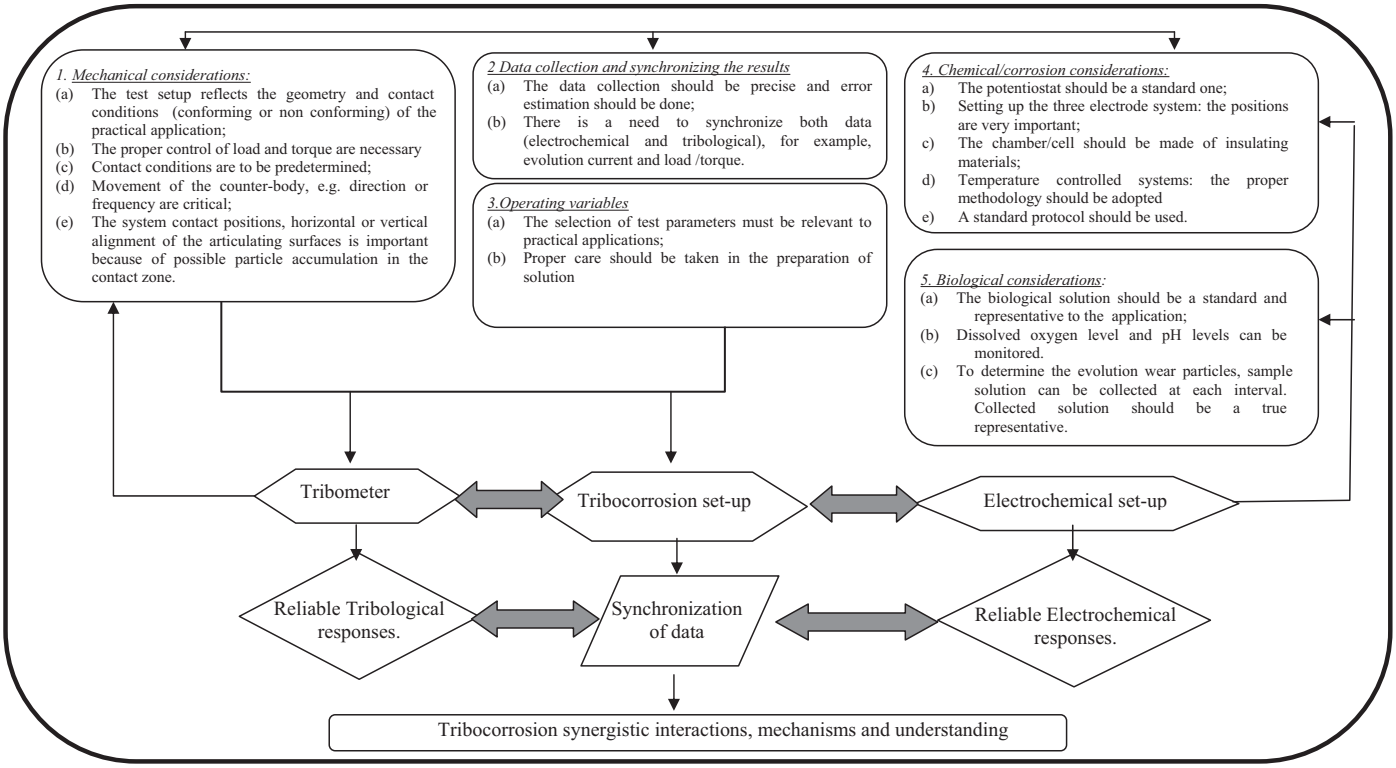

References

[1] D. Landolt, M. Stemp, S. Mischler, Electrochemical methods in tribocorrosion – a critical appraisal, Electrochim. Acta 46 (2001) 3913–3929.
[2] R.J.K. Wood, Tribo-corrosion of coatings: a review, J. Phys. D: Appl. Phys. 40 (2007) 5502–5521.
[3] D. Landolt, Electrochemical and materials aspects of tribocorrosion systems, J. Phys. D: Appl. Phys. 39 (2006) 3121–3127.
[4] S. Mischler, S. Debaud, D. Landolt, Wear-accelerated corrosion of passive metals in tribocorrosion systems, J. Electrochem. Soc. 145 (3) (1998) 750–758.
[5] S. Mischler, P. Ponthiaux, A round robin on combined electrochemical and friction tests on alumina/stainless steel contacts in sulphuric acid, Wear 248 (2001) 211–225.
[6] J.-P. Celis, P. Pontiaux, F. Wenger, Tribocorrosion of materials: interplay between chemical, electrochemical and mechanical reactivity of surfaces, Wear 261 (2006) 939–946.
[7] S. Mischler, Triboelectrochemical technique and interpretation methods in tribocorrosion: a comparative evaluation, Tribol. Int. 41 (2008) 573–583.
[8] F.W. Chan, J.D. Bobyn, J.B. Medley, J.J. Krygier, M. Tanzer, Wear and lubrication of metal-on-metal hip implants, Clin. Orthop. Relat. Res. 369 (1999) 10–24 (CHECK format).
[9] J.J. Jacobs, J.L. Glibert, R.M. Urban, Current concepts review: corrosion of metal orthopaedic implants, J. Bone Joint Surg. 80-A (2) (1998).
[10] H. Willert, G.H. Buchhorn, A. Fayyazi, R. Flury, M. Windler, G. Koster, C.H. Lohmann, Metal-on-metal bearings and hypersensitivity in patients with artificial hip joints, J. Bone Joint Surg. 87-A (1) (2005).
[11] J.J. Jacobs, N.J. Hallab, R.M. Urban, M.A. Wimmer, Wear particles, J. Bone Joint Surg. 88-A (2.) (2006).
[12] R.M. Urban, J.J. Jacobs, M.J. Tomlison, J. Gavriloc, J. Black, M. Peoch, Dissemination of wear particles to the liver, spleen and abdominal lymph nodes of patients with hip and knee replacements, J. Bone Joint Surg. 82-A (4.) (2000).
[13] M.A. Wimmer, J. Loos, R. Nassutt, M. Heitkemper, A. Fischer, The acting wear mechanisms on metal-on-metal hip joint bearings – in vitro results, Wear 250 (2001) 129–139.
[14] M.A. Wimmer, C. Sprecher, R. Hauert, T. ger, G.A. Fischer, Tribochemical reaction on metal-on-metal hip joint bearings – a comparison between in vitro and in vivo results, Wear 255 (2003) 1007–1014.
[15] C.N. Kraft, B. Burian, O. Diedrich, M.A. Wimmer, Implications of orthopedic fretting corrosion particles on skeletal muscle microcirculation, J. Mater. Sci.: Mater. Med. 12 (2001) 1057–1062.
[16] Ch. Kaddick, M.A. Wimmer, Hip simulator wear testing according to the newly introduced standard ISO 14242, Proc. Inst. Mech. Engrs. Part H 215 (2001) 429–442.
[17] J. Geringer, B. Forest, P. Combrade, Fretting-corrosion of materials used as orthopedic implants, Wear 259 (2005) 943–951.
[18] N.J. Hallab, C. Messina, A. Skipor, J.J. Jacobs, Difference in the fretting corrosion of metal–metal and ceramic–metal modular junctions of total hip replacements, J. Orthop. Res. 22 (2004) 250–259.
[19] J.A. Hendry, R.M. Piliar, The fretting corrosion resistance of PVD surface-modified orthopedic implant alloys, J. Biomed. Res. (Appl. Biomater.) 58 (2001) 156–166.
[20] Y. Yan, A. Neville, D. Dowson, Biotribocorrosion of CoCrMo orthopedic implant materials – assessing the formation and effect of the biofilm, Tribol. Int. 40 (2007) 1492–1499.
[21] D. Sun, J.A. Wharton, R.J.K. Wood, L. Ma, W.M. Rainforth, Microabrasion–corrosion of cast CoCrMo alloy in simulated body fluids, Tribol. Int. 42 (1) (2009) 99–110.
[22] M.M. Stack, M.T. Mathew, H. Jawan, On the construction of microabrasion maps for a steels/polymer couple in corrosive environment, Tribol. Int. 38 (9) (2005) 848–856.
[23] K.L. Dahm, P.A. Dearnley, Abrasion response and abrasion–corrosion interactions for coating on biomedical stainless steel, Wear 259 (2005) 933–942.
[24] M.M. Stack, K. Chi, Mapping sliding wear of steels in aqueous, condition, Wear 255 (2003) 456–465.
[25] Y. Yan, A. Neville, D. Dowson, S. Williams, J. Fisher, Tribocorrosion, analysis of wear and metal ion release interactions from metal-on-metal and ceramic-on-metal contacts for the application in artificial hip prostheses, Proc. I MechE Part J: J. Eng. Tribol. 222 (3) (2008) 483–492.
[26] P.-Q. Wu, J.-P. Celis, Electrochemical noise measurements on stainless steel during corrosion-wear in sliding contacts, Wear 256 (2004) 480–490.
[27] P. Ponthiaux, F. Wenger, D. Drees, J.-P. Celis, Electrochemical techniques for studying tribocorrosion processes, Wear 256 (2004) 459–468.
[28] J.-P. Celis, P. Ponthiaux, F. Wenger, Tribo-corrosion of materials: interplay between chemical, electrochemical, and mechanical reactivity of surfaces, Wear 261 (9) (2006) 939–946.
[29] A.K. Basak, P. Matteazzi, M. Vardavoulias, J.-P. Celis, Corrosion-wear behaviour of thermal sprayed nanostructred FeCu/WC–Co coatings, Wear 261 (2006) 1042–1050.
[30] A.C. Vieira, A.R. Ribeiro, L.A. Rocha, J.P. Celis, Influence of pH and corrosion inhibitors on the tribocorrosion of titanium in artificial saliva, Wear 261 (2006) 994–1001.
[31] A. Berradja, F. Bratu, L. Benea, L. Willems, J.-P. Celis, Effect of sliding wear on tribocorrosion behaviour of stainless steels in a ringer solution, Wear 261 (2006) 987–993.
[32] M. Stemp, S. Mischler, D. Landolt, The effect of mechanical and electrochemical parameters on the tribocorrosion rate of stainless steel in sulphuric acid, Wear 255 (2003) 466–475.
[33] S. Barril, N. Debaud, S. Mischler, D. Landolt, Influence of fretting regimes on the tribocorrosion behaviour of Ti6Al4V in 0.9 wt.% sodium chloride solution, Wear (2004) 256.
[34] J. Stojadinovic, D. Bouvet, M. Declercq, S. Mischeler, Effect of electrode potential on the tribocorrosion of tungsten, Tribol. Int. 34 (2001) 599–608.
[35] S. Barril, S. Mischler, D. Landolt, Influence of fretting regimes on the tribocorrosion behaviour of i6Al4V in 0.9 wt.% sodium chloride solution, Wear 256 (2004) 963–972.
[36] S. Mischler, A. Spiegel, M. Stemp, D. Landolt, Influence of passivity on the tribocorrosion behavior of carbon steel in aqueous solutions, Wear 251 (2001) 295–307.
[37] F. Galliano, E. Galvanetto, S. Mischler, D. Landolt, Tribocorrosion behavior of plasma nitrided Ti–6Al–4V alloy in neutral NaCl, Solut. Surf. Coat Technol. 145 (2001) 121–131.
[38] M. Azzi, J.A. Szpunar, Tribo-electrochemical technique for studying tribocorrosion behavior of biomaterials, Biomol. Eng. 24 (2007) 443–446.
[39] L. Duisabeau, P. Combrade, B. Forest, Environmental effect on fretting of metallic materials for orthopedic implants, Wear 256 (2004) 805–816.
[40] M.T. Mathew, L.A. Rocha, E. Ariza, F. Vaz, A.C. Fernandes, P. Carvalho, TiCxOy thin films for decorative applications Tribocorrosion Mechanism, Tribol. Int. 41 (7) (2008) 603–615.
[41] S.C. Ferreira, E. Ariza, L.A. Rocha, J.R. Gomes, P. Carvalho, F. Vaz, A.C. Fernandes, et al., Tribocorrosion behaviour of ZrO_xN_y thin films for decorative applications, Surf. Coat. Technol. 200 (22–23) (2006) 6634–6639.
[42] R. Pourzal, A. Fischer, Reciprocating Sliding Wear of Surface Modified Austenitic High Nitrogen Stainless Steel and CoCrMo-alloy, in: A. Fischer, K. Bobzin (Eds.), Friction, Wear and Wear Protection, Wiley-VCH, 2008.
[43] I. Serre, N. Celati, R.M. Pradeilles-Duval, Tribological and corrosion wear of graphite ring against Ti_6Al_4V disk in artificial seawater, Wear 252 (2002) 711–718.
[44] M. Morita, T. Sasada, I. Normura, Y.Q. Wei, T. Tsukamoto, Influence of low dissolved oxygen concentration in body fluid on corrosion fatigue behaviors of implant metals, Ann. Biomed. Eng. 20 (5) (1992) 505–516.
[45] R. Buscher, et al., Subsurface microstructure of metal-on-metal hip joints and its relationship to wear particle generation, J. Biomed. Mater. Res. B: Appl. Biomater. 72B (2005) 206–214.
[46] H. Yoshida, et al., Three-dimensional hip contact area and pressure distribution during activities of daily living, J. Biomech. 39 (2006) 1996–2004.
[47] M.M. Stack, J. Rodling, M.T. Mathew, H. Jawan, W. Huang, G. Park, C. Hodge, Micro-abrasion corrosion of a CoCr/UHMWPE couple in ringer solution: an approach to construction of mechanism and synergism maps for the application to bio-implants, Wear 269 (2010) 376–382.
[48] M.A. Wimmer, R. Nassutt, F. Lampe, E. Schneider, M.M. Morlock, A new screening method designed for wear analysis of bearing surfaces used in total hip arthroplasty, in: J.J. Jacobs, T.L. Craig (Eds.), Alternative Bearing Surfaces in Total Joint Replacement, American Society for Testing Materials, 1998, pp. 30–43, ASTM STP 1346.